Pergamon

Geochimica et Cosmochimica Acta, Vol. 62, No. 19/20, pp. 3307–3321, 1998

0016-7037/98 $19.00 + .00

PII S0016-7037(98)00239-7

The Qinglongshan oxygen and hydrogen isotope anomaly near Donghai in Jiangsu Province, China

DOUGLAS RUMBLE,*[,1] and T.-F. YUI[2]

[1]Geophysical Laboratory, 5251 Broad Branch Road, Washington, D.C. 20015, USA
[2]Institute of Earth Sciences, Academia Sinica, Taipei, Taiwan

(*Received October* 15, 1997; *accepted in revised form July* 14, 1998)

Abstract—The Qinglongshan isotope anomaly has unusually low values of both $\delta^{18}O$ and δD. Grnets from coesite-bearing eclogite are as low as −11‰ (VSMOW) and rutiles are −15‰. Phengites have δD of −120‰ (VSMOW). The low values were acquired in an ancient geothermal system prior to subduction during Triassic continental collision. New data shows that depleted isotope values in different rock types extend over distances of 20 × 40 km demonstrating that the geothermal system retained structural coherence throughout subduction and exhumation. The finding of structural coherence suggests that not only eclogites, with their characteristic ultra-high pressure mineral assemblages, but also gneisses, meta-granites, and meta-sediments were all subjected to metamorphism in the coesite-eclogite facies. Oxygen isotope fractionation between quartz and garnet gives estimates of peak metamorphic temperatures at 754–893°C. The spatial extent of oxygen isotopic equilibration between different rock types was limited to tens of centimeters. The persistence of hydrous minerals such as epidote and phengite approaching high temperature oxygen isotope exchange equilibrium with ultrahigh pressure minerals in coesite-bearing rocks shows that mineral-bound water can be subducted into the upper mantle. *Copyright © 1998 Elsevier Science Ltd*

1. INTRODUCTION

The Qinglongshan oxygen and hydrogen isotope anomaly is defined by unusually low values of $\delta^{18}O$ and δD in metamorphic minerals. Garnets, omphacites, and epidotes from eclogites are as low as −11‰ in $\delta^{18}O$ and rutiles even lower at −15‰. Phengites have $\delta^{18}O$ values of −10‰ and δD extends to −120‰. The rarity of such isotopic values — their shock effect—may be appreciated by comparison with compilations of data for metamorphic quartz and hydrous minerals (Sharp et al., 1993; their Figs. 8 and 9). Qinglongshan quartz, at −7‰ $\delta^{18}O$, is 12‰ lower than the lowest posted value (out of a total range of variation of 25‰), and phengites are at the extreme low end of the distribution in δD for hydrous minerals (Sharp et al., 1993). Blattner et al. (1991, 1997) report low $\delta^{18}O$ analyses of −13‰ for contact metamorphosed andesites but Qinglongshan marks the lowest record for eclogites thus far. Since the announcement of the discovery of low ^{18}O values at the First International Eclogite Workshop, Stanford University, in 1994 (Yui et al., 1994; Baker et al., 1994) there has been intensive research on the rocks (Yui et al., 1995, 1997; Zheng et al., 1996; 1998; Baker et al., 1997).

The significance of the low isotopic values does not lie in their ephemeral existence as a world's record for eclogite, however. The isotopic geochemistry of Qinglongshan is remarkable for the fidelity with which protolith depositional conditions have been preserved. Their preservation is all the more astonishing when it is realized that the rocks survived subduction to depths of 75 km, metamorphism at that depth under ultra-high pressure (UHP) (coesite-forming) conditions, and exhumation to the surface. The significance of the Qinglongshan anomaly is that its well-preserved protolith characteristics are a benchmark against which subsequent tectonic and metamorphic effects can be measured.

Previous investigations showed that protolith basalts and sandstones of the area were at or near the Earth's surface and were subjected to alteration by meteoric water, in a geothermal system, prior to subduction (Yui et al., 1995, 1997; Baker et al., 1997; Zheng et al., 1996, 1998). New data reported herein demonstrates that: (1) A wide variety of rock types including meta-granites, schists, and gneisses in addition to previously described eclogites and quartzites have depleted $\delta^{18}O$ values. (2) Minerals from rocks of different mineralogical and isotopic composition failed to equilibrate in respect to oxygen isotopes over distances as short as a few meters during UHP metamorphism. Intermineral fractionations of $^{18}O/^{16}O$ are consistent, however, with the attainment of grain-scale isotopic exchange equilibrium, (or at least communication), between minerals in mutual contact under UHP conditions. But mineral pairs have subsequently re-equilibrated during cooling from peak metamorphic temperatures. (3) The discovery that a variety of different rock types are isotopically depleted suggests that the surrounding UHP metamorphic terrain, including host gneisses, meta-granites, and eclogites, retained structural coherence throughout continental collision, UHP metamorphism, and exhumation over an area of at least 20 by 40 km. Meta-granites with $\delta^{18}O$ of quartz as low as –2.5‰ may represent the heat engine that powered the ancient geothermal system. (4) The provisional conclusion that there was no isotopic exchange between crustal rocks and the upper mantle into which they were subducted is supported by the new data. Data in the form of sample traverses across lithologic contacts at a scale of centimeters to meters as well as regional mapping of the anomaly at a scale of kilometers will be presented below supporting these interpretations.

*Author to whom correspondence should be addressed (rumble@gl.ciw.edu).

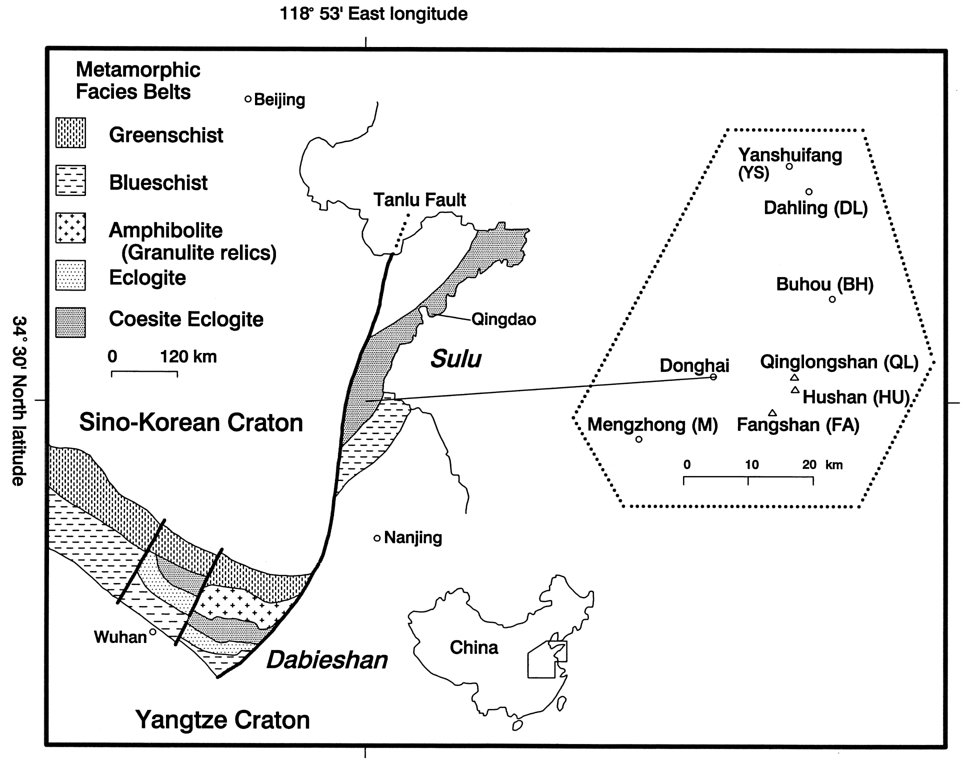

Fig. 1 Metamorphic facies belts of E. China and Tanlu Fault. Inset map shows location of Qinglongshan, Donghai, and sample locations mentioned in text. Two scale bars show scale of main map and inset, respectively.

2. LOCATION AND GEOLOGY

Qinglongshan, in Northern Jiangsu Province, is a low ridge extending NNE-SSW for several kilometers with outcrops of eclogite flanked by quartz-feldspar-amphibole gneiss to the west (Figs. 1, 2). The ridge is surrounded by flat plains planted in bean fields. The lower part of its eastern slope is a cemetery. Hushan and Fangshan, both underlain by meta-granitic rocks with mafic segregations, are higher ridges to the SSW (Figs. 1, 2). Both have been quarried extensively and provide well-dressed stone to build handsome homes in nearby villages.

Qinglongshan is located at the southern end of the Sulu UHP metamorphic terrain (Fig. 1). The terrain extends 500 km from northern Jiangsu province to the northeast tip of the Shandong peninsula. Sulu was separated from the Dabieshan UHP terrain in the Cretaceous by 500 km left-lateral displacement on the Tanlu (Tancheng-Luijiang) strike-slip fault (Xu, J., 1993; Wang, Q. et al., 1996). Coesite, diagnostic of UHP metamorphism, is widespread in Sulu as inclusions in garnet, omphacite, kyanite, and epidote (Yang and Smith, 1989; Enami and Zang, 1990; Hirajima et al., 1990; Hirajima et al., 1992; Hirajima et al., 1993; Enami et al., 1993; Wang et al., 1993; Wang, X. et al., 1995; Zhang et al., 1995; Zhang and Liou, 1997). Intergranular coesite is known from one locality in Sulu (Liou and Zhang, 1996; Ye et al., 1996). The UHP terrains of Dabieshan and Sulu lie along the common boundary separating the Archaen Sino-Korean craton to the North from the Proterozoic Yangtze craton to the South. The suture between the two tectonic plates is occupied by the Qingling-Tongbai-Dabieshan-Sulu orogenic belts, only the latter two of which are known to contain UHP rocks. Continental collision, subduction, and metamorphism took place in the Triassic followed by exhumation and widespread intrusion of Cretaceous granites (Wang, Q. et al., 1996). The Sulu terrain includes quartz-feldspar-biotite gneiss, amphibolite, marble, metamorphosed granites, eclogite, metasedimentary, and ultramafic rocks. Of these, UHP mineral assemblages have been found in garnetiferous peridotite and pyroxenite, eclogite, meta-granitoids, and meta-sedimentary kyanite quartzite and garnet-quartz-jadeite rock (Enami and Zang, 1988; Hirajima et al., 1993; Yang et al., 1993; Enami et al, 1993; Zhang et al., 1994; Zhang et al, 1995; Zhang et al., 1995). Apart from Cretaceous granite intrusions 25 km to the west, post-collisional geologic history in the vicinity of Qinglongshan is represented by isolated erosional remnants of Tertiary basalt flows and a gaping unconformity at the base of the Quaternary sedimentary cover.

The geologic age of UHP metamorphism at Qinglongshan has been dated by measuring Sm-Nd and Rb-Sr mineral and whole rock isochrons (Li et al., 1994; Li, 1996) and by analyzing U-Pb systematics in zircons (Ames et al., 1996). A mineral-whole rock isochron including the UHP minerals garnet, omphacite, and phengite from Qinglongshan eclogite gives a Sm-Nd age of 226.3 $\pm$ 4.5 Ma and a Rb-Sr age of 219.5 $\pm$ 0.5 Ma (Li et al., 1994; Li, 1996). Zircon ages are 217 $\pm$ 9 Ma (lower discordia intercept) and 762 $\pm$ 28 Ma (upper intercept) (Ames et al., 1996). Thus, three independent geochronometers agree on the age of UHP metamorphism at Qinglongshan as 217–226 Ma. The protolith age of 762 $\pm$ 28 Ma is less precisely known, however, because the zircon chord on a

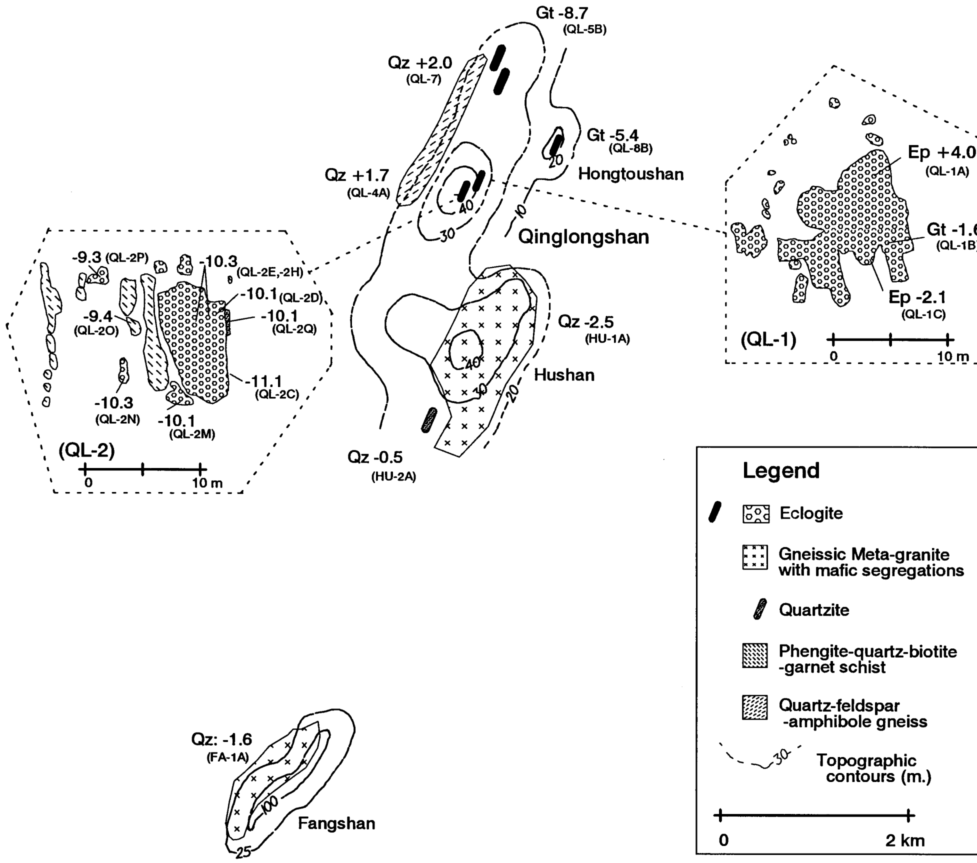

Fig. 2. Outcrop map, sample localities (in parenthesis), and topography of the Qinglongshan area. Inset maps show two summit outcrops, QL-1 and QL-2. Values of $\delta^{18}O$ of garnet plotted for QL-2. Other $\delta^{18}O$ values designated as Gt = garnet, Ep = epidote, Qz = quartz. Separate scale bars given for main map and inset maps.

discordia plot is dominated by metamorphic ages (Ames et al., 1996). Phengite from Qinglongshan yields $^{40}Ar/^{39}Ar$ plateau ages of 876.5 $\pm$ 15.9 Ma (Li et al., 1994). Paradoxically, despite its older apparent radiometric age, phengite textures in the analyzed sample suggest it grew later than garnet, omphacite, and rutile, perhaps during exhumation. The source of excess ^{40}Ar is thought to have been the K- and ^{40}Ar-rich Proterozoic leucocratic country gneisses (Li et al., 1994).

The age of eclogite country rocks from Qinglongshan has not been measured radiometrically. Samples of felsic gneiss from the northern Sulu UHP terrain give poorly defined zircon discordia ages of 177 $\pm$ 45 Ma, (lower intercept) and 782 $\pm$ 32 Ma (upper intercept; Ames et al., 1996). Gneisses from Dabieshan have lower intercepts of 219–227 Ma and upper intercepts of 772–854 Ma (Ames et al., 1996; Rowley et al., 1997). It is assumed that both metamorphic and protolith ages of Qinglongshan gneisses and metagranites are similar to those measured in northern Sulu and Dabieshan.

3. METHODS

Most samples were collected from weathered surface outcrops. In some of these the feldspars, biotite, and phengite appear altered in thin section. The freshest samples of gneiss, meta-granites, and mafic segregations were found in working quarries at Hushan and Fangshan (Fig. 2). Unweathered eclogite was obtained from drill cores recovered from drill holes ZK 703 (samples M-1A and M-1G), ZK 2304 (M-2A), and ZK-2302 (M-3A) near Maobei-Mengzhong (Fig. 2), access to which was graciously provided by the Donghai County Geology Team of Jiangsu Province. Samples were collected by D. Rumble, R. Zhang, and K. Ye in August, 1995. Tape and compass maps of the Qinglongshan summit outcrops were surveyed by Y. Ogasawara and J. G. Liou. Regional mapping was controlled by Y. Ogasawara with a portable GPS receiver.

Minerals were analyzed for oxygen isotopes with a CO_2 laser fluorination system in the Geophysical Laboratory similar to that of Sharp (1990) but differing in that O_2 gas is analyzed directly in the mass spectrometer without conversion to CO_2 (Rumble and Hoering, 1994). Reported values of $\delta^{18}O$ are averages of duplicate or triplicate determinations with a precision of 0.1–0.2‰. The accuracy of the measured isotope ratios may be assessed by comparing the results of Zheng et al. (1996) obtained by conventional fluorination (Clayton and Mayeda, 1963), and those of Yui et al. (1995) with the laser system, on analyzed minerals from kyanite quartzite from the Qinglongshan summit outcrop. In the list that follows, $\delta^{18}O$ values for each mineral are given in pairs, (e.g., laser, conventional), the first of which is from Yui et al. (1995) Table 1, sample SQ) and the second from Zheng et al. (1996), Table 1, sample QL95-8): quartz (-7.3, -7.1), phengite (-8.8, -8.9), kyanite (-9.1, -8.9), epidote (-10.1, -9.5), and garnet (-10.3, -10.3). Additional validation of analytical results for oxygen isotopes is given by observing that a total of 277 analyses of UHP minerals and two tank O_2 standard gases give a least squares regression with slope 0.518 ($R^2 = 0.9998$) on a plot of $\delta^{18}O$ vs.$\delta^{7}O$, in good agreement with the 0.52 slope of the terrestrial fractionation line (Clayton, 1993). Hydrogen isotope analyses of phengite were conducted by T.F. Yui in the Institute of Earth Sciences, Academia Sinica, Taipei, Taiwan. The

Table 1. $\delta^{18}O_{VSMOW}$ values of minerals (‰), rock types and alteration

	Rock	Qz[1]	Pl	Bt	Ky	Ph	Am	Gt	Ep	Om	Rt	Cc	Alteration[5]
BH-1A[2]	eclg[3]							6.4					
BH-1D	eclg							8.2					
DL-1A	eclg							3.7					
FA-1A	m-grt	−1.6	−3.0	−6.9									
FA-1B	seg	−1.1											
FA-1C	seg		−1.3	−6.0									
HU-1A	seg	−2.5		−6.1					−5.6				
HU-1B	m-grt	−2.4	−3.8	−6.5									
HU-1C	m-grt	−2.3	−4.3	−7.7									
HU-2A	qtzite	−0.5			−1.5								
M-1A	eclg							0.3		−0.4			
M-1G	eclg							1.9	1.8				
M-2A	gn	3.2	2.1				−1.1	0.0					
M-3A	gn	4.5	4.5										
QL-1A	ep-eclg								4.0				Ph
QL-1B	ep-eclg	0.8			−0.5	−1.2		−1.6	−2.4	−2.2	−5.3		
QL-1C	ep-eclg								−2.1				
QL-2C	am-eclg					−10.0	−11.0	−11.1	−11.1	−11.1	−14.8		Om
QL-2D	eclg							−10.1	−9.9	−10.1	−14.1		Om
QL-2E	eclg					−9.4		−10.3	−10.8	−11.2	−14.2		
QL-2H	eclg							−10.3		−10.4	−14.1		vein
QL-2M	eclg	−7.7				−10.7		−10.1	−10.4	−10.7	−14.6		
QL-2N	eclg					−9.3		−10.3	−10.1	−10.0			Om
QL-2O	sh	−6.5	−2.4			−9.0		−9.4					
QL-2P	eclg					−8.9		−9.3	−9.0	−8.6	−13.4		Om, Ph
QL-2Q	qtzite	−7.4				−9.7			−10.1				Ph, Ky
QL-3A	alt-grt	−2.8							−8.1				
QL-3B	vein											−3.0(−0.3)[4]	
QL-4A	gn	1.7	0.5										
QL-5A	eclg							−8.7	−8.4	−9.2	−12.4		Om
QL-5B	eclg							−8.7					
QL-5C	eclg							−7.6					Om
QL-6B	eclg							−6.3	−6.3	−6.4	−9.9		
QL-7	GN	2.0					−1.1						
QL-8A	eclg					−4.3		−4.9		−5.6	−8.2		
QL-8B	eclg					−4.6		−5.4		−5.5	−8.7		
YS-1	eclg							−5.4		−5.9			

[1] Minerals: QZ = quartz, Pl = plagioclase, BT = biotite, Ky = kyanite, Ph - phengite, Am = amphibole, Gt = garnet, Ep = epidote, Om = omphacite, Rt = rutile, Cc = calcite.
[2] Localities: BH = Buhou, DL = Dahling, FA = Fangshan, HU = Hushan, M = Mengzhong, QL = Qinglongshan, YS = Yanshuifang.
[3] Rock: -eclg = eclogite, mn-grt = meta-granite, seg = mafic segregation, qtzite = quartzite, gn = gneiss, ep-eclg = epidote-eclogite, am-eclg = amphibole-eclogite, sh = schist, alt-grt = altered granite.
[4] Value in parenthesis is $\delta^{13}C_{VPDB}$.
[5] Names of altered minerals and whether secondary vein is present.

D/H measurements were obtained with the method of Godfrey (1962) and a precision of ±3‰ is estimated.

4. NOTATION

Isotope data are reported as parts per thousand differences from a reference standard. The δ notation is defined as

$$\delta_x = \frac{R_x - R_{STD}}{R_{STD}}(1000)$$

where R_x and R_{STD} are the isotope ratios $^{18}O/^{16}O$ or D/H ($^2H/^1H$) of the sample (x) and standard (STD), respectively. Data for oxygen and hydrogen are reported relative to VSMOW (Vienna Standard Mean Ocean Water) (Coplen, 1995).

5. PETROGRAPHY

Minerals separated from hand samples of a variety of rock types including gneiss, eclogite, and meta-granitoid were analyzed for $\delta^{18}O$. (The discussion follows the abbreviated rock names of Table 1.)

5.1. Eclogite: (abbreviated eclg in Table 1)

The primary mineral assemblage is garnet + omphacite + phengite + rutile ± epidote ± kyanite ± barrosite ± quartz ± quartz pseudomorph after coesite. The rocks show a gneissic layering and volumetric proportions of minerals are non-uniform on a scale of centimeter, thick layering. In most samples omphacite is altered to a symplectic rim of plagioclase + sodic augite. More rarely, kyanite is rimmed by albite and secondary white mica.

5.2. Epidote–eclogite: (ep-eclg, Table 1)

The primary assemblage is the same as eclogite, however, large porphyroblasts of epidote (1–2 cm in length) cross-cut gneissic layering and contain inclusions of all the primary minerals. Symplectic alteration rims of plagioclase and sodic augite are common on omphacite. This rock type is distinctive in the field and was found without other rock types at only one locality (QL-1, Fig. 2).

5.3. Amphibole–eclogite: (am-eclg, Table 1)

Amphibole–eclogite consists of the primary eclogite assemblage with 1-cm barrosite porphyroblasts cross-cutting foliation. Omphacite is rimmed by plagioclase and sodic augite in most samples. Amphibole – eclogite is interlayered with eclogite at locality QL-2 (Fig. 2).

5.4. Gneiss: (abbreviated gn, Table 1)

The gneiss is exposed in water-filled pits extending 2 km NNE-SSW along the west flank of Qinglongshan (Fig. 2). Outcrops of gneiss are deeply weathered and their contacts are not exposed. The primary assemblage is plagioclase + microcline + quartz + hornblende + sphene + magnetite + monazite + ilmenite ± garnet with a strong gneissic foliation. Weathering alteration appears as hematite replacing magnetite along octahaedral (111) faces and leucoxene rimming sphene.

5.5. Meta-granite: (m-grt, Table 1)

Unweathered, weakly foliated meta-granite consisting of plagioclase + microcline + quartz + epidote + biotite + monazite + magnetite ± garnet crops out over a distance of at least 7 km in quarries on Hushan and Fangshan (Fig. 2). Contacts between the meta-granite and its wall rocks were not found. Relatively unaltered meta-granite is present in other UHP localities. Meta-granite in contact with coesite-bearing eclogite has been reported from Yangkou (Hirajima et al., 1993), 250 km northeast of Qinglongshan. The coesite-bearing, pyrope quartzite from Dora Maira is present as lenses within granitic orthogneiss (Compagnoni et al., 1995). The meta-granite of this study, however, does not show the intensity of mineralogical alteration reported from the other localities.

5.6. Mafic segregations: (seg, Table 1)

Mafic segregations with assemblages of biotite + epidote + hornblende + plagioclase + microcline + quartz ± garnet ± sphene occur as lenses in meta-granite on Hushan and Fangshan (Fig. 2). Texturally similar mafic segregations are present in the meta-granite of Dora Maira (Tilton et al., 1997; Fig. 3).

5.7. Schist: (sh, Table 1)

A phengite + quartz + plagioclase + biotite + garnet schist is found in 2 m thick layers in contact with eclogite on Qinglongshan (Fig. 2). The schist contains a surprisingly oxidized sub-assemblage of rutile + ilmeno-hematite (hematite with exsolution lamellae of ilmenite) (Rumble, 1973).

5.8. Quartzite: (qtzite, Table 1)

Quartzite occurs as a 0.5 m thick layer in contact with eclogite on Qinglongshan and in an excavation south of Hushan (Fig. 2). The primary assemblage is quartz + phengite + epidote + kyanite + garnet + rutile. Secondary replacement consists of kyanite rimmed concentrically by white mica and albite. Phengite is rimmed by biotite.

5.9. Altered gneiss and vein: (alt-gn, vein, Table 1)

Altered gneiss and a vein of massive calcite were found in a pit on the eastern slope of Qinglongshan. The gneiss consists of relict primary plagioclase, sphene, and apatite with secondary subhedral epidote, calcite, and radiating sheaves of fine-grained chlorite. The vein has rhomboid calcite crystals up to 6 cm on a side with a thin mantle of dark green chlorite.

6. RESULTS

6.1. Isotopic Equilibration versus the Persistence of Differences in Protolith Composition

The persistence of differences in protolith stable isotope composition throughout a complete collisional cycle of subduction, metamorphism, and exhumation is a known feature of medium- and high-pressure rocks from amphibolite and blueschist facies terrains (Anderson, 1967; Taylor and Coleman, 1968; Sheppard and Schwarcz, 1970; Rumble, 1978; Rumble and Spear, 1983; Chamberlain and Conrad, 1991; Bebout, 1991; Wickham and Peters, 1992; Todd and Evans, 1993). What these and other workers have observed is the failure of a mineral such as quartz to achieve uniform oxygen isotopic composition across contacts between rocks differing in whole rock isotopic composition. The spatial extent of isotopic equilibration during metamorphism may be measured quantitatively by collecting millimeter- to centimeter-scale sample profiles perpendicular to rock contacts and analyzing mineral separates. Recognition of gradients in isotopic composition has been exploited in a number of studies to obtain estimates of the magnitude of material flux across contacts between dissimilar rock types (Lassey and Blattner, 1988; Baumgartner and Rumble, 1988; Ganor et al., 1989; Bickle and Baker, 1990; Jamtviet et al., 1992; Bowman et al., 1994; Baker and Spiegelman, 1995; Gerdes et al., 1995; Bickle et al., 1997; Abart and Sperb, 1997). These investigations have made valuable contributions to understanding metamorphism because they have established whether fluids were present and free to infiltrate lithologic boundaries. Thus, it is appropriate to search outcrops of UHP rocks for gradients in isotopic composition in order to test for the presence or absence of infiltrating water. The persistence of recognizable differences in isotopic composition denies pervasive infiltration across lithologic contacts of exotic fluids strongly out of equilibrium with protoliths. If such infiltration had occurred it would have homogenized isotopic compositions (Ganor et al., 1996; Matthews et al., 1996).

Pre-metamorphic differences in isotopic composition between rock types are present throughout the Qinglongshan region. The eclogite outcrop belt shows both along- and cross-strike changes in garnet composition from −11.1 δ^{18}O‰ (QL-2C) at Qinglongshan summit to +8.2 at Buhou (BH-1D), +3.7 at Dahling (DL-1A), and –5.4 at Yanshuifang (YS-1) over a distance of 30 km in a North-South direction (Fig. 3, Table 1). Eclogite is flanked to the west by quartz-feldspar-amphibole gneisses with quartz values of +1.7 to +2.0‰ (Samples QL-4A, and QL-7) (Fig. 4; Table 1). The metamorphosed granites and mafic segregations of Hushan and Fangshan, to the South, have depleted values of −1.6 to −2.5‰ δ^{18}O in quartz (samples FA-1A, HU-1A) (Fig. 3). A traverse from West to East, 25 km across the region, shows gneisses with quartz of +3.2 to +4.5‰ and eclogites with garnets of +0.3 to +1.9 in the Maobei-Mengzhong drill hole (drill holes ZK 703, 2302, and 2304, samples M-1A, M-1G, M-2A, M-3A), Qinglongshan summit eclogites with quartz of –7.4 and garnet of –11.1, followed by Hongtoushan eclogite (QL-8A, 8B) with garnet of –5.4 δ^{18}O (Fig. 4, Table 1).

Qinglongshan rocks record a number of examples of persistent pre-metamorphic differences in $^{18}O/^{16}O$ composition at the scale of single outcrops. Rocks separated by several meters did not equilibrate. Eclogite garnets from the summit outcrop are mostly homogeneous at −10.2‰ δ^{18}O but one sample at the east end of the outcrop is −11.1‰ (QL-2C) and another at the west end is −9.3‰ (QL-2P) (Fig. 2,4). A phengite-quartz-biotite-garnet schist (QL-2O) interlayered with eclogite has garnet at −9.4‰ δ^{18}O (Fig. 2, 4). A second outcrop 30 m east

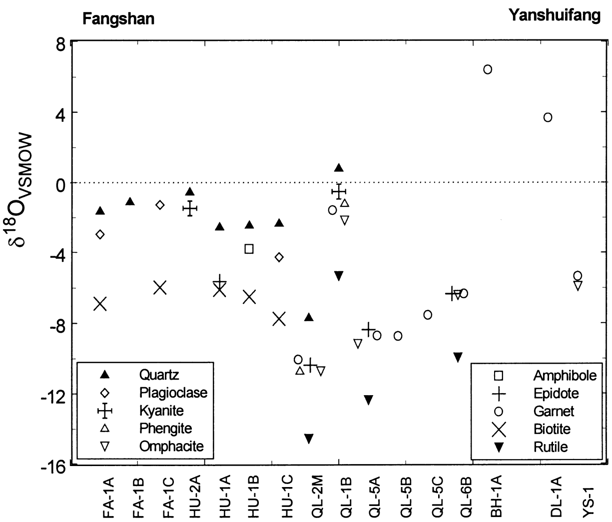

Fig. 3. South to north profile of $\delta^{18}O_{VSMOW}$ values of coexisting minerals with sample numbers.

of the summit has epidotes from eclogite that range from +4 (QL-1A) to −2.4 (QL-1B)‰ over a distance of 3 m (Fig. 2, 4; compare Zheng et al., 1998). Qinglongshan rocks in close proximity to each other, however, such as schist (QL-2O) and eclogite (QL-2P) or kyanite quartzite and eclogite (Yui et al, 1995; Zheng et al., 1996) have almost identical mineral $\delta^{18}O$ values (Fig. 2, 4). Qinglongshan rocks are not alone among HP and UHP examples in their failure to attain oxygen isotope equilibrium between dissimilar lithologies. Baker et al. (1997) found in the UHP Dabieshan terrain garnets from small eclogite pods enclosed in marble with $\delta^{18}O$ as high as +9.5 to +11‰ but garnet from a nearby 3 m thick eclogite boudin was 2.3. Examples of oxygen and carbon isotopic disequilibrium across rock contacts in high pressure (HP) and ultra-high pressure terrains are reported by Sharp et al. (1993) and Getty and Selverstone (1994).

The length scale of hydrogen isotope equilibration across lithologic contacts appears to be somewhat longer than that for

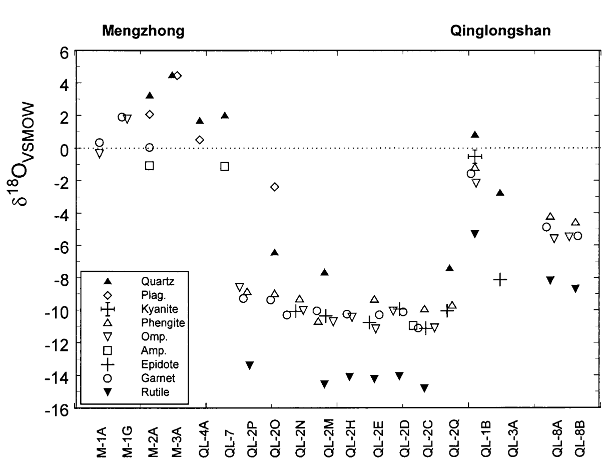

Fig. 4. West to east profile of $\delta^{18}O_{VSMOW}$ values of coexisting minerals with sample numbers.

Table 2. Values of δD and $\delta^{18}O$ for phengite

	δD	$\delta^{18}O$
BH-5D	−55	7.9[b]
DL-1C	−87	5.3[b]
QL-1	−113	−9.0[a]
QL-1B	−124	−1.2
QL-1C	−121	−1.5[b]
QL-1F	−124	
QL-2C	−104	−10.0
QL-2E	−101	−9.4
QL-2O	−105	−9.0
QL-2Q	−106	−9.7
QL-6B	−127	−5.7[b]
QL-8A	−123	−4.3
QL-8B	−118	−4.6
QL-8C	−123	
SQ-92-3	−114	−8.8[a]

[a] Yui, et al. 1995;
[b] Estimated from average mineral-mineral fractionations (Table 3.)

oxygen isotopes but conclusions are less certain because fewer samples were analyzed for D/H than for $^{18}O/^{16}O$. Eclogites QL-2C (−10.0‰) and QL-2P (−8.9‰) have phengites differing in $\delta^{18}O$ by 1.1‰, a significant discrepancy given analytical uncertainties of 0.15‰. The δD values of the phengites, however, −104‰ (QL-2C) and −106‰ (QL-2P), are indistinguishable (± 3 ‰) (Table 2). The entire summit outcrop (QL-2C, 2E, 2O, 2P, 2Q) is uniform at δD of −101 to −106‰. Three nearby outcrops, QL-1, Hongtoushan (QL-8), and QL-6 are lower at δD of −118 to −127‰. Phengites from Buhou and Dahling, however, are considerably heavier at δD of −55 and −87‰, respectively, reflecting their heavy $\delta^{18}O$ values of +6.4 to + 8.2‰ (garnet, BH-1A, -1D) and + 3.7 (DL-1A) (Table 2). Zheng et al. (1998) give a smaller range of variation in δD, from –104 to −83‰.

The differences in protolith oxygen and hydrogen isotopic composition are thought to have arisen owing to local differences in the intensity of geothermal alteration. Observed isotopic alteration in fossil hydrothermal systems is known to be influenced by water/rock ratio, temperature, proportion of meteoric vs. magmatic water, proximity to permeable fracture zones, and superposition of successive hydrothermal events (Taylor, 1974). For example, Sheppard and Taylor (1974) list sericite analyses from the Butte, Montana, hydrothermal ore deposit that range from –10 to +10‰ in $\delta^{18}O$ and –175 to –110‰ in δD.

6.2. Oxygen Isotope Geothermometry

The measurement of oxygen isotope partitioning between coexisting minerals to estimate paleo-temperatures has the potential to quantify the thermal conditions of metamorphism (Clayton and Epstein, 1961). To realize this potential, much effort has been expended to complete laboratory calibration of oxygen isotope fractionation between commonly occurring pairs of rock-forming minerals (Chiba et al., 1989; Clayton et al., 1989; Zheng et al., 1994; Rosenbaum and Mattey, 1995; Chacko et al., 1996). Parallel work on calibration has included empirical observation of natural mineral pairs (Bottinga and Javoy, 1975; Sharp, 1995; Sharp and Kirschner, 1994) and theoretical calculations (Kieffer, 1982; Clayton and Kieffer, 1991; Zheng, 1991, 1993). Nevertheless, when application of oxygen isotope geothermometry is made to metamorphic rocks, it is frequently observed that pairs of minerals from the same hand specimen give discordant temperature estimates (Deines, 1977) and, furthermore, disagree with mineralogical geothermometers. Among the reasons advanced to explain discrepant temperatures are (1) failure of minerals to attain isotope exchange equilibrium under metamorphic conditions; (2) inaccurate calibration of temperature dependence of fractionation; and (3) down-temperature re-equilibration, that is, continued exchange of isotopes between minerals as rocks cool during exhumation (Giletti, 1986). Each of these factors will be evaluated below in interpreting geothermometric results from Qinglongshan.

6.2.1. *Failure to equilibrate under peak metamorphic conditions.*

It was shown, above, that there is a tendency for dissimilar rocks separated by more than one meter to fail to equilibrate during UHP metamorphism. The observation does not, however, disqualify Qinglongshan rocks as candidates for successful geothermometry. The scale of equilibration required to record temperatures is that of single mineral grains in mutual contact over millimeter or submillimeter distances. Thus, sampling small volumes of visibly homogeneous rock for mineral separates, as was done in this study, should promote the likelihood of obtaining minerals in mutual equilibrium. One should note, however, that taking mineral separates from thinly layered and gneissic rocks may sample across differences in bulk oxygen isotope composition. Supporting the hypothesis of an approach to mineral-mineral equilibrium at Qinglongshan is a systematic order of enrichment in ^{18}O, e.g., quartz $>$ (phengite, kyanite) $>$ (epidote, clinopyroxene, garnet, amphibole) $>$ rutile despite differences in bulk (^{18}O and mineralogy from sample to sample (Figs. 3, 4). Comparing mineral-mineral fractionations measured in this study with published values reveals discrepancies for garnet-phengite, garnet-epidote, and garnet-omphacite (Table 3). Garnet-phengite varies from –0.6 (this study) to –1.2 to –1.5 (Yui et al., 1995; Zheng et al., 1996, 1998) to –1.9 (1000ln α) in Dabieshan (Zheng et al., 1998) and the Western Gneiss region (Agrinier et al., 1985). Garnet-epidote ranges from 0.1 (this study) to –1.2 (1000ln α) in the Western Gneiss region (Agrinier et al., 1985). The compiled data illustrates that mineral pairs like garnet-epidote and garnet-phengite have small and rather variable fractionations. Given an analytical precision of 0.15‰ on each mineral analysis, it may be seen that pairs of these minerals are unlikely to provide precise geothermometry. Mineral pairs with larger fractionations such as quartz-omphacite, quartz-garnet, quartz-epidote, quartz-rutile, quartz-biotite, and garnet-rutile are more appropriate. Among the latter group, quartz-omphacite, quartz-epidote, and quartz–garnet are relatively consistent but quartz-rutile, quartz-biotite, and garnet-rutile fractionations are irregular (Table 3).

Observations of regular or irregular fractionations are not sufficient in themselves to establish isotopic equilibrium or its failure. Other data are useful in evaluating mineral pairs. Omphacite is vulnerable to retrograde mineralogical alteration and is commonly rimmed by symplectites of plagioclase + sodic augite or sodic plagioclase + Ca-amphibole + epidote (Zhang et al., 1995). Yui et al. (1997) found a correlation between disequilibrium garnet-omphacite ^{18}O/^{16}O fractionations and symplectic alteration. Whether the correlation is due to retrograde isotopic exchange or the difficulty of separating omphacite from symplectite with rigorous purity is difficult to assess. The minerals phengite and epidote are undoubtedly bona fide members of UHP assemblages in many eclogites (Liou et al., 1995). At Qinglongshan, however, epidote grows across gneissic foliation and includes garnet, omphacite, rutile, quartz, and coesite (or coesite pseudomorphs). Some phengites crosscut foliation suggesting growth following the primary assemblage. Routine mineral separation schemes would fail utterly to purify different generations of the same minerals. Kyanite is rimmed concentrically by white mica and albite. Feldspar and biotite are typically susceptible to both retrograde isotopic exchange and mineralogical alteration.

Examples of clear-cut oxygen isotope disequilibrium are obvious, especially in country-rock gneisses and meta-granitoids: sample QL-2O has a large, reversed quartz-plagioclase fractionation; sample QL-3A, a heavily metasomatized gneiss, shows a quartz-epidote fractionation larger than other samples. The quartz-feldspar-garnet-phengite schist interlayered with eclogite at Qinglongshan summit (sample QL-2O) has feldspar enriched by 4 ‰ in δ^{18}O relative to coexisting quartz (Fig. 4, Table 1, 3). The phengites of the rock are the most inhomogeneous analyzed. Here is an example of the effects of normal waters when they gain access to rocks depleted in ^{18}O. Gneiss (QL-3A) pervasively penetrated by vein calcite (QL-3B) is exposed in a pit on the east slope of Qinglongshan (Fig. 4). Quartz-epidote fractionation in the gneiss is at variance with those measured in other rock types but consistent with mineralogical evidence of post-metamorphic metasomatism and gives an apparent temperature of 361°C (Table 3, 4), (calibration of Matthews, 1994). The quartz-biotite partitioning values of the Hushan and Fangshan meta-granitoids range from 3.6 to 5.4 corresponding to an apparent temperature difference of some 150°C (Table 3, 4).

6.2.2. *Inaccurate calibration of geothermometers*

Comparison of temperature estimates based on different calibrations of oxygen isotope geothermometers provides a direct evaluation of the accuracy of thermometry. Results presented in Table 4 compare empirical-theoretical (Javoy, 1977) calibrations with experimental determinations by various investigators (Matthews, 1994; Rosenbaum and Mattey, 1995; Chacko et al., 1996). Differences in temperature estimates are as high as 90°C for quartz–phengite and 150°C for quartz-biotite. Thermometric estimates using the calibrations of Zheng (1991, 1993) give 650–765°C for quartz-garnet, 655–760°C for quartz-omphacite, 595–725°C for quartz-phengite, and 390–510°C for quartz-rutile from Qinglongshan (Zheng et al., 1998; Table 1).

Additional evaluation of accuracy of geothermometry may be made by comparing isotopic thermometry with mineral chemistry thermometry. Typical values of mineral thermometers from Sulu eclogites are 750°C ($\pm$50°C) at 30 kbars and for

Table 3. Mineral-mineral fractionations

Sample	Qz-Pl	Qz-Ph	Qz-Ky	Qz-Om	Qz-Ep	Qz-Gt	Qz-Bt	Qz-Rt	Gt-Ky	Gt-Ph	Gt-Ep	Gt-Om	Gt-Rt
FA-1A	1.33						5.27						
HU-1A					3.11		3.58						
HU-1B	1.36						4.08						
HU-1C	1.94						5.44						
HU-2A			0.94										
M-1A												0.69	
M-1G											0.12		
M-2A	1.14					3.16							
M-3A	0.02												
QL-1B		2.02	1.35	2.99	3.21	2.40		6.16	−1.06	−0.38	0.81	0.58	3.76
QL-2C										−1.17	0.01	−0.02	3.74
QL-2D											−0.18	−0.05	3.99
QL-2E										−0.95	0.48	0.87	4.00
QL-2H												0.20	3.90
QL-2M		3.06		3.05	2.71	2.39		6.96		0.67	0.31	0.66	4.57
QL-2N										−0.98	−0.23	−0.28	
QL-2O	−4.08	2.58				2.94				−0.36			
QL-2P										−0.41	−0.25	−0.69	4.17
QL-2Q		2.31			2.65								
QL-3A					(5.39)								
QL-4A	1.15												
QL-5A											−0.35	0.47	3.69
QL-6B											−0.01	0.07	3.63
QL-8A										−0.64		0.73	3.34
QL-8B										−0.83		0.05	3.30
YS-1												0.57	
Average		2.5	1.1	3.0	2.9	2.7	4.6	6.6		−0.6	0.1	0.3	3.8
Std. Dev.		0.4	0.3		0.3	0.4	0.9	0.6		0.6	0.4	0.5	0.4
Qinglongshan[1]		1.46	1.81		2.77	2.98			−1.16	−1.51	−0.20	−0.24	
Qinglongshan[2]		1.92	1.85	2.37	2.42	3.13			−1.31	−1.21	−0.81	−0.71	
Qinglongshan[3]		2.10	1.87	2.27	3.54	3.53		7.44	−1.67	−1.43	−0.06	−1.26	3.73
Dabieshan[4]												0.89	
Dabieshan[5]										−0.43			
Dabieshan[3]		2.12		2.56	3.00	3.79		5.74		−1.86	−0.70	−1.23	1.95
Dora Maira[6]		2.02	2.25			2.82	4.78	4.83	−0.56	−0.80			2.02
Western Gn.[7]		1.78		2.48		2.98	2.68	4.82		−1.89	−1.20	−0.54	1.77
Tauern Wind.[8]		2.50						6.66					
Sesia Zone[9]		2.73		3.29			6.75						
Europe[10]				2.86	3.24	3.64		6.47			−0.45	−0.50	2.87

[1] Yui et al., 1995;
[2] Zheng et al., 1996;
[3] Zheng et al., 1998;
[4] Yui et al., 1997;
[5] Baker et al., 1997;
[6] Sharp et al., 1993;
[7] Western Gneiss Region, Agrinier et al., 1985;
[8] Tauern Window, Matthews, 1979;
[9] Desmons and O'Neil, 1978;
[10] Vogel and Garlick, 1970.
Mineral abbreviations as in Table 1. Std. Dev. = standard deviation.

garnet peridotites 850°C (±50°C) at 40–60 kbars. Zhang et al. (1995) used Fe-Mg partitioning between garnet and clinopyroxene in eclogites to calculate temperatures of 685–830° (Powell, 1985) or 710–850°C (Ellis and Green, 1979) at a pressure of 30 kb, as indicated by the presence of coesite. The same geothermometer was used by Enami et al. (1993) to obtain 650–850°C for $P < 26$ to 28 kb and by Hirajima et al. (1992) to find 740°C (±60°C) for $P > 28$ kb. Intersections of P-T curves plotted by Yang et al. (1993) for olivine-garnet (O'Neill and Wood, 1980), orthopyroxene-garnet (Carswell and Harley, 1990), clinopyroxene-garnet (Krogh, 1988), and Al in orthopyroxene (Nickel and Green, 1985; Brey and Kohler, 1990) give 750–900°C at 45–50 kb for mineral rims and 800–1200°C at 50–70 kb for cores in garnet peridotites. Zhang et al. (1994) estimated peak temperatures of 822–920°C at 39 kb for Donghai ultramafic rocks.

In summary, quartz-garnet oxygen isotopic and mineralogical geothermometers overlap in the range 725–875°C, consistent with an approach to isotopic exchange equilibrium between UHP minerals at high temperature. There is significant disagreement between experimental, theoretical, and empirical calibrations for a number of geothermometers, however. Resolution of the problem of discordant temperatures requires not only consideration of analytical uncertainties and inaccuracies

Table 4. Selected temperature estimates

	Qz-Pl[1]	Qz-Bt[2]	QZ-BT[3]	Qz-Ep[4]	Qz-Gt[5]	Qz-Ph[2]	Qz-Ph[3]	Qz-Om[6]	Qz-Am[2]	Qz-Rt[7]	Qz-Rt[3]	Gt-Rt[7]
FA-1A	647	520	375									
HU-1A		666	500	562								
HU-1B	637	615	450									
HU-1C	490	509	360									
M-2A	719				725				555			
QL-1B				548	872	643	550	610		630	580	455
QL-2C												456
QL-2D												434
QL-2E												432
QL-2H												441
QL-2M				622	875	502	400	600		576	525	387
QL-2O					762	558	475					
QL-2P												418
QL-2Q				632		596	500					
QL-3A				361								
QL-4A	714											
QL-5A												461
QL-6B												467
QL-7									687			
QL-8A												499
QL-8B												504

Geothermometer calibrations: [1]Javoy, 1977, $Z_{An} = 0.15$; [2] Javoy, 1977; [3]Chacko et al., 1996; [4] Matthews, 1994, $X_{Ps} = 0.22$; [5] Rosenbaum and Mattey, 1995; [6] Matthews, 1994, $X_{Jd} = 0.4$; [7] Matthews, 1994.

in the calibration of isotope fractionations but also evaluation of the role of post-metamorphic, down-temperature oxygen isotope exchange.

6.2.3. *Post-metamorphic, down-temperature oxygen isotope exchange*

Temperature estimates given in Table 4 show that certain mineral pairs, such as quartz-garnet, record higher apparent temperatures than other pairs such as quartz-rutile. Discordant temperatures are the rule rather than the exception in many metamorphic rocks (Deines, 1977). In a pioneering study, Giletti (1986) showed that diffusive re-equilibration of oxygen isotopes between minerals during cooling from metamorphic temperatures may produce strongly discordant apparent temperatures. Among the controls on diffusive re-equilibration are the speed of oxygen diffusion in minerals (magnitudes of activation energy and pre-exponential factor), cooling rate, grain size, and mineral abundances, as well as inter-mineral isotope partitioning. A number of theoretical models of diffusion-dominated isotopic re-equilibration have been proposed and applied to natural examples (Eiler et al., 1992, 1994; Jenkin et al., 1994; Massey et al., 1994; Sharp and Moecher, 1994; Farquhar et al., 1996; Ghent and Valley, 1998). The results of model calculations are highly specific to each rock investigated; nevertheless, it is evident that re-equilibration during cooling can produce the entire range of discordant temperatures observed in natural samples, including the reversal of equilibrium partitioning. A common theme of experimental research is the role of water in accelerating oxygen diffusion in minerals (Elphick et al., 1988; Sharp et al., 1991; Watson and Cherniak, 1997). Dry rocks are more likely to record higher apparent temperatures than wet rocks, a concept graphically portrayed in the phrase hydrothermal quench (G. R. T. Jenkin, pers. commun.). According to this idea, a high temperature metamorphic rock that had been thoroughly dehydrated by mineral reactions would preserve its high temperature oxygen isotope intermineral fractionations more faithfully than a rock with wet grain boundaries.

An example of a model calculation of re-equilibration in epidote-eclogite sample QL-1B is given in Fig. 5 for a cooling rate of 75°C/my (cf. Gebauer et al., 1997) using the Fast Grain Boundary (FGB) model of Eiler et al. (1992, 1994). It may be seen that garnet, epidote, and kyanite remain unchanged in composition throughout cooling. Rutile and omphacite change composition initially but close to further isotopic exchange at 600°C. Phengite retains its high temperature composition over the first 150°C of cooling but, upon the closure of rutile and omphacite, it begins to decrease in $\delta^{18}O$. Quartz gains ^{18}O and loses ^{16}O continually as the rock cools. In eclogites lacking quartz, the computed behavior is different in that phengite increases, rutile decreases, barrosite decreases slightly and garnet, omphacite, and epidote are unchanged. Choosing faster cooling rates, larger grain sizes, and dry diffusion coefficients results in higher closure temperatures. Slower cooling, finer grain size, and wet diffusion coefficients give lower closure temperatures. No combination of variables was found in the models, including a search for a specific cooling rate, that reproduced measured isotopic compositions within analytical uncertainty. The predictions of model calculations agree qualitatively, if not quantitatively, with observations. Qinglongshan eclogites have variable quartz-phengite fractionations of 2 to 3 ($1000\ln\alpha$), low quartz-rutile temperatures, and garnet-omphacite fractionation reversals. The high quartz-garnet temperatures are puzzling, however, in view of the computed behavior in which garnet remains unchanged but quartz increases in $\delta^{18}O$, which should lead to lower apparent temperatures. Test calculations comparing the Fast Grain Boundary (FGB) model of Eiler et al. (1994) and the Giletti (1986) model embodied in

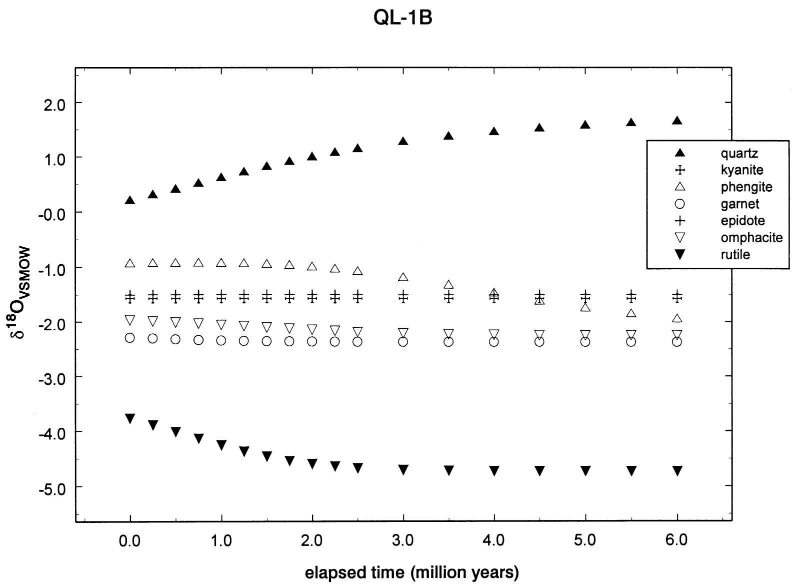

Fig. 5. Diffusional re-equilibration of eclogite (QL-1B) during cooling from 850° to 400°C at a cooling rate of 75°C per million years (cooling rate after Gebauer et al., 1997). Whole rock $\delta^{18}O$ values calculated from modal abundances and analyzed mineral compositions. Fast Grain Boundary model of Eiler et al. (1992,1994). Diffusion data of Giletti and Yund,1984; Farver and Giletti, 1985; Fortier and Giletti, 1989; Farver, 1989; Fortier and Giletti, 1991; Sharp et al., 1991; and Moore et al., in press. Diffusion parameters for kyanite and epidote calculated after Fortier and Giletti (1989) (cf. Ghent and Valley, 1997).

program COOL (Jenkin et al., 1994) show qualitatively similar behaviors except that COOL closure temperatures are generally higher. The tentative nature of the calculations should be emphasized especially as there is no experimental data available on diffusion coefficients and pre-exponential factors for UHP minerals within some 25 kilobars of coesite-eclogite facies conditions.

6.2.4 *Evaluation of oxygen isotope geothermometry*

Previous studies (Yui et al., 1995; Zheng et al., 1996, 1998) concluded that the minerals of Qinglongshan had attained high temperature oxygen isotope exchange equilibrium during UHP metamorphism. The results of the present investigation suggest a more cautious conclusion. The data are consistent with an approach to grain-scale oxygen isotope equilibrium under UHP conditions but this is seen through an obscuring veil of diffusional re-equilibration and retrograde metamorphism. It has to be admitted that there are as yet no uniquely definitive conclusions to be made regarding the application of oxygen isotope geothermometry to Qinglongshan rocks. Failure to equilibrate during prograde metamorphism, erroneous calibration of fractionation, diffusional re-equilibration during exhumation, retrograde mineralogical alteration, as well as analytical errors all may contribute to uncertainties in temperature estimates. Each rock sample or outcrop must be evaluated in relation to mineral reaction textures and tectonic history in order to interpret geothermometric data. In this study quartz-garnet mineral pairs give apparent temperatures most consistent with overall petrologic and tectonic evidence. The recording of high temperatures by quartz-garnet pairs is consistent with rapid cooling of rocks with dry grain boundaries (Giletti, 1986; Eiler et al., 1992,1994; Jenkin et al., 1994; Sharp and Moecher 1994; Farquhar et al., 1996). Geodynamic models of continental collision, subduction, and exhumation combined with the preservation of minerals susceptible to alteration such as coesite suggest that UHP terrains were exhumed rapidly under dry conditions. Prediction by the FGB and COOL models of specific patterns of $^{18}O/^{16}O$ zonation within individual mineral grains as a consequence of diffusional re-equilibration during exhumation offers a new means of achieving a more definitive interpretation of geothermometry. The advent of in situ oxygen isotope analysis (Eiler et al., 1995; Wiechert et al., 1995; Rumble et al., 1997) brings the promise of measuring isotope zoning and distinguishing between calculated models of cooling behavior.

7. GEOLOGICAL IMPLICATIONS

Qinglongshan rocks failed to achieve oxygen isotope equilibrium over distances as short as 1 m across lithologic contacts. Qinglongshan minerals, however, approached high temperature oxygen isotope equilibrium at the scale of millimeter-sized grains. These contrasting behaviors are the basis for drawing inferences about the geologic age at which the depleted isotopic signature was acquired and about the environment of protoliths. Grain-scale equilibration between UHP minerals of anomalous isotopic composition under high temperature conditions demonstrates that depletion in ^{18}O and D was imposed prior to metamorphism (Yui et al. 1995, 1997; Zheng et al., 1996, 1998; Baker et al., 1997). The persistence of premetamorphic differences in isotopic composition between different rock types throughout the collisional cycle suggests that information on protolith conditions survives to the present.

7.1. Protolith Environment

The low $\delta^{18}O$ and δD values of eclogites and their country rocks in Table 1 record that UHP protoliths were once at or near Earth's surface and were subjected to alteration in a geothermal area charged with meteoric water from high paleolatitude or high paleoaltitude. Groundwater from a cold climate, recharged by rain, melted snow, or glacier ice is the only plausible reservoir with sufficiently low $^{18}O/^{16}O$ and D/H ratios to accomplish the observed alteration (Craig, 1961; Taylor, 1974). Seawater is too enriched in ^{18}O and D as are waters from continental and oceanic crust and the mantle to be viable as potential agents of alteration (Yui et al., 1995, 1997; Zheng et al., 1996,1998; Baker et al., 1997). The proposed origin of the Qinglongshan oxygen and hydrogen isotope anomaly resembles that deduced for many younger and less intensely metamorphosed terrains. Depletions in ^{18}O and D are present in contact aureoles of high latitude epizonal plutons (Taylor, 1974) and in batholiths (Magaritz and Taylor, 1976). Negative values of $\delta^{18}O$ in basaltic rocks and associated intrusives are known from the North Atlantic Igneous Province (Hattori and Muehlenbachs, 1982; Brandriss et al., 1995; Nevle et al., 1994). The lowest published $\delta^{18}O$ for metamorphic rocks are from contact metamorphosed volcanics from the former South Polar region of Gondwanaland (Blattner et al., 1997). In the reported examples, meteoric water from cold climates was responsible for isotopic exchange. Subjacent intrusives, epizonal, or batholithic plutons supplied the heat necessary to drive water circulation and permit isotopic exchange to proceed detectably.

7.2. Structural Coherence

Deducing the internal structure of UHP rocks is important because of the light it may shed on the physical mechanisms by which continental collision, subduction, and exhumation is accomplished. Mapping the structure of the UHP rocks at Qinglongshan is difficult because outcrops are widely scattered, and many are deeply weathered. Furthermore, available outcrops show isolated occurrences of rock types such as quartzite and eclogite embedded in a rather unremarkable matrix of gray gneisses and meta-granites lacking distinctive marker horizons. The observed depletion in ^{18}O and D of geothermal alteration provides a most welcome and needed pre-metamorphic benchmark against which subsequent deformation can be measured.

An ancient geothermal system, preserved in Qinglongshan UHP metamorphic rocks, is the chief isotopic evidence of structural coherence. Despite tectonic disruption that accompanied subduction and exhumation, isotopic evidence of geothermal alteration remains recognizable over an area of 20 by 40 km. The westernmost outcrops known with low $\delta^{18}O$ values are from the Maobei-Mengzhong drill core (drill holes ZK-703, -2302, and -2304) with quartz at $+3.2‰$ (M-2A) in quartz-feldspar gneiss and garnets in eclogite at 0 (M-2A) to $+1.9‰$ (M-1G; Fig. 1, 4; Table 1). Low ^{18}O rocks extend 40 km North-South from Fangshan through Hushan and Qinglongshan to Yanshuifang (Fig. 1) with quartz from meta-granite at -1.6 (FA-1A) at Fangshan, quartz at Hushan with -2.4 (HU-1B), and, far to the North, eclogite garnets with $-5.4‰$ (YS-1) at Yanshuifang (Fig. 1, 3; Table 1). Structural coherence has also been demonstrated by Baker et al. (1997) who report isotopic evidence of a fossil hydrothermal system in the Dabieshan UHP terrain, remarkably similar to the one from Sulu described herein. The Dabieshan terrain has ^{18}O depletions as low as $-5.5‰$ in eclogite and -6.8 in country rock gneisses. The area of unusually low $\delta^{18}O$ values measures 15 by 25 km. A regional view of the scale of structural coherence recorded by isotopic data may be obtained by restoring approximately 500 km of Cretaceous left-lateral displacement on the Tanlu Fault (Fig. 1). The UHP terrains of Sulu and Dabieshan are contiguous, once restoration has been made, and the ancient geothermal areas are made whole, as well. The length scale of the reunified geothermal areas is now seen to be 100 km; that is the sum of 25 km in Dabieshan (Baker et al., 1997), 50 km separating Qinglongshan from the trace of the Tanlu Fault, and 25 km North and South beyond Qinglongshan. It is emphasized that geochemical mapping with stable isotopes in Dabieshan and Sulu is incomplete, thus, estimates of the length scale of structural coherence are to be understood as preliminary minimum values.

The combined Dabieshan-Qinglongshan oxygen and hydrogen isotope anomaly is comparable to well-known geothermal systems such as the Idaho Batholith, as reviewed by Criss and Taylor (1986). The Cretaceous Idaho Batholith is intruded by a number of Eocene epizonal plutons, extending over a North-South distance of more than 150 km. Each of the younger plutons is the center of concentric zones of progressively more intense hydrothermal alteration. Oxygen isotope values of feldspar vary from –7 to $+10$ $\delta^{18}O$ and hydrogen isotopes of biotite from –170 to –70 δD. Note that the pattern of lateral heterogeneity in $\delta^{18}O$ and δD seen at Qinglongshan is repeated in Idaho and is attributed to local disparities in water-rock ratios caused by highly anisotropic variations in permeability.

The most convincing evidence of structural coherence undoubtedly is supplied by geologic mapping and structural analysis. The isotopic evidence is useful in that it supports the hard work of field mapping. Xue et al. (1996) mapped a crystalline, folded nappe no more than a few kilometers thick, cut above and below by thrust faults and extending over 10 by 10 km in the Dabieshan UHP terrain. Sample traverses across the nappe show three areas in which garnets from eclogite, amphibolite, and country-rock gneisses have unusually low $\delta^{18}O$ of -5 to 0‰ (Baker et al., 1997, Fig. 3, p.1688). A thrust-bounded coherent slab of UHP eclogite, marble, quartzite, schist, and gneiss is at Shuanghe, Dabieshan (Cong et al., 1995). The slab has been offset by a late, right lateral fault and is truncated by a Mesozoic granite intrusion so its maximum extent cannot be determined. The slab is now exposed over a strike length of 1 km with a width of 0.2 km.

The interpretation of structural coherence detailed above has implications for the ongoing debate about whether UHP metamorphism is allochthonous or in situ. Proponents of an allochthonous origin cite the sheared contacts of eclogite pods and the failure of enclosing gneiss mineral assemblages to record the high pressures of eclogite assemblages as evidence that eclogites were subjected to UHP metamorphism before tectonic emplacement into their presently exposed hosts (Smith, 1995; see reviews of Coleman and Wang, 1995; Harley and Carswell, 1995; Cong and Wang, 1996; Krogh and Carswell, 1995; and Schreyer, 1995). In contrast, advocates of the in situ hypothesis note the presence of high pressure mineral relics in host gneisses (Wang, X. et al., 1995), identical ages of metamorphism for host and eclogites measured radiometrically (Ames et al., 1996; Li, 1996; Rowley et al., 1997), and geologically mapped, structurally coherent units in UHP terrains (Compagnoni et al., 1995; Cong et al., 1995; Michaud et al., 1995; Xue et al., 1995). Stable isotopic evidence of structural coherence supports the in situ hypothesis. Baker et al. (1997; Fig. 5) found a virtually one-to-one correspondence between the δ^{18}O of eclogite garnets and that of host gneisses, a relationship inconsistent with the proposed tectonic juxtaposition of low pressure gneisses and high pressure eclogites. The results of this study are in accord with the in situ hypothesis, as well. The Qinglongshan eclogite belt, which contains quartz as low as -7‰ δ^{18}O (QL-2M, -2O, -2Q), is flanked to the west by quartz-feldspar-amphibole gneisses with $+1.7$ to $+2.0$‰ quartz (QL-4A, -7) and to the southeast by meta-granitoids with -1.1 to -2.5‰ quartz (FA-1B, HU-1A; Fig. 2; Table 1). It should be recognized that even positive values of $+1.7$ to $+2.0$ are unusually low for gneisses of metasedimentary origin. Negative values of -1.1 to -2.5 for meta-granitoids are still more unusual. Thus, the entire Qinglongshan terrain is an artifact of a relict geothermal system, an isotopically coherent whole that has not been dismembered tectonically.

8. SUMMARY AND CONCLUSIONS

The preservation of an ancient geothermal system with distinctive oxygen and hydrogen isotope composition demonstrates that slabs of UHP rocks at Qinglongshan retained structural coherence throughout the orogenic cycle. The isotopic evidence also shows the UHP metamorphism to be in situ, not allochthonous; that is, adjacent protoliths experienced UHP metamorphism at the same time and under similar pressure-temperature conditions. Neither the maximum lateral extent, the thickness of Qinglongshan's coherent UHP slabs, nor the structures (presumably faults) bounding the slabs are known. The 5 km deep scientific drill hole planned by the Chinese Academy of Geological Sciences at Maobei (near Mengzhong, Fig. 1) will provide definitive information on slab thickness and bounding structures by direct sampling (Prof. Xu Zhiqin, pers. commun.).

Given that the length scale of oxygen isotope equilibration across lithologic contacts between UHP rocks was less than 3 m, it is clear that no isotopic exchange could have taken place between subducted crustal rocks and the upper mantle. The closest pristine mantle samples are xenoliths in Neogene volcanics erupted along the Tanlu fault. Clinopyroxene from the xenoliths has δ^{18}O of $+5.5$ to $+5.8$ (Xu,Y.G. et al., 1996) in comparison to omphacites with -10 to -11‰ at Qinglongshan.

The data do not support the presence of a pervasive fluid free to infiltrate across lithologic contacts during metamorphism. The persistence of pre-metamorphic differences in isotopic composition between dissimilar rock types indicates the lack of flowing fluid to mediate isotope exchange. The preservation of high-temperature oxygen isotope fractionations between UHP minerals indicates dry, not wet conditions after the peak of metamorphism. The dramatic effects of retrograde isotope alteration, discussed above, as well as retrograde mineral reactions illustrate the devastating impact on these rocks when fluids gain access to them following UHP metamorphism. The indicated fluid-rock behavior is consistent with a model of metamorphism in which fluid is present only episodically, when released by dehydration reactions. Fluids do not remain at reaction sites but are driven away by buoyancy, facilitated by reaction- and deformation-enhanced permeability (Rumble, 1994). The coexistence of the hydrous minerals epidote and phengite approaching oxygen isotope exchange equilibrium with UHP assemblages of garnet, omphacite, and kyanite, demonstrates that water chemically bound in minerals can be transported to depths of at least 75–100 km into the upper mantle.

Acknowledgements—Prof. Bolin Cong and Dr. Qingchen Wang (Chinese Academy of Sciences) gave an informative introduction to Dabieshan UHP geology and provided advice and practical assistance without which the study could not have been completed. Mineral separates of high quality were prepared by the Hebei Geology Team through the good offices of B. Cong and Q. Wang. Prof. J. G. Liou and Dr. R. Y. Zhang (Stanford University) and Dr. Y. Ogasawara (Waseda University) were of material assistance in the field. Their wise counsel on UHP metamorphism was indispensable. We are grateful to Dr. Kai Ye (Chinese Academy of Sciences) for logistical support in the field. The discussion of geothermometry was substantially improved through the advice of B. Hacker (UC Santa Barbara), J. Eiler (California Institute of Technology), G. R. T. Jenkin (University of Leicester), Z. D. Sharp (University of New Mexico), and E. D. Young (Oxford University). Eiler and Jenkin kindly supplied executable versions of their computer models. Research was supported by NSF EAR 9526700.

REFERENCES

Abart R. and Sperb R. (1997) Grain-scale stable isotope disequilibrium during fluid-rock interaction; 1: Series approximations for advective-dispersive transport and first-order kinetic mineral-fluid exchange. *Amer. J. Sci.* **297,** 679–706.

Agrinier P., Javoy M., Smith D. C., and Pineau F. (1985) Carbon and oxygen isotopes in eclogites, amphibolites, veins, and marbles from Western Gneiss Region, Norway. *Chem. Geol.* **52,** 145–162.

Ames L., Zhou G., and Xiong B. (1996) Geochronology and isotopic character of ultrahigh-pressure metamorphism with implications for collision of the Sino-Korean and Yangtze cratons, central China. *Tectonics* **15,** 472–489.

Anderson A. T. (1967) The dimensions of oxygen isotopic equilibrium attainment during prograde metamorphism. *J. Geol.* **75,** 323–332.

Baker J., Matthews A., Mattey D., Xue F., and Rowley D. B. (1994) Fluid infiltration during ultra-high pressure metamorphism, Dabie Shan, China. In *First Workshop on UHP Metamorphism* (ed. J. G. Liou et al.), pp. A-75. Stanford Univ. Press.

Baker J. and Spiegelman M. (1995) Modelling an infiltration-driven geochemical front. *Earth Planet. Sci. Lett.* **136,** 87–96.

Baker J., Matthews A., Mattey D., Rowley D. B., and Xue F. (1997) Fluid-rock interaction during ultra-high pressure metamorphism, Dabie Shan, China. *Geochim. Cosmochim. Acta* **61,** 1685–1696.

Baumgartner L. P. and Rumble D. (1988) Transport of stable isotopes: I: Development of a kinetic continuum theory for stable isotope transport. *Contrib. Mineral. Petrol.* **98,** 417–430.

Bebout G. E. (1991) Geometry and mechanisms of fluid flow at 15 to 45 kilometer depths in an early Cretaceous accretionary complex. *Geophys. Res. Lett.* **18,** 923–926.

Bickle M. J. and Baker J. (1990) Advective-diffusive transport of isotopic fronts: An example from Naxos, Greece. *Earth Planet. Sci. Lett.* **97,** 78–93.

Bickle M. J., Chapman H. J., Ferry J. M., Rumble III D., and Fallick A. E. (1997) Fluid flow and diffusion in the Waterville Limestone, South-Central Maine: Constraints from strontium, oxygen, and carbon isotope profiles. *J. Petrol.* **38,** 1489–1512.

Blattner P. and Williams J. G. (1991) The Largs high-latitude oxygen isotope anomaly (New Zealand) and climatic controls of oxygen isotopes in magma. *Earth Planet. Sci. Lett.* **103,** 270–284.

Blattner P., Grindley G. W., and Adams C. J. (1997) Low ^{18}O terranes tracking Mesozoic polar climates in the South Pacific. *Geochim. Cosmochim. Acta* **61,** 569–576.

Bottinga Y. and Javoy M. (1975) Oxygen isotope partitioning among the minerals in igneous and metamorphic rocks. *Rev. Geophys. Space Phys.* **13,** 401

Bowman J. R., Willett S. D., and Cook S. J. (1994) Oxygen isotopic transport and exchange during fluid flow; one-dimensional models and applications. *Amer. J. Sci.* **294,** 1–55.

Brandriss M. E., Nevle R. J., Bird D. K., and O'Neil J. R. (1995) Imprint of meteoric water on the stable isotope compositions of igneous and secondary minerals, Kap Edvard Holm Complex, East Greenland. *Contrib. Mineral. Petrol.* **121,** 74–86.

Brey G. P. and Kohler T. (1990) Geothermobarometry in four-phase lherzolites. II-New thermobarometers and practical assessment of existing thermobarometers. *J. Petrol.* **31,** 1353–1378.

Carswell D. A. and Harley S. L. (1990) Mineral barometry and thermometry. In *Eclogite Facies Rocks* (ed. D. A. Carswell), pp. 83–110. Blackie and Son

Chacko T., Hu X., Mayeda T. K., Clayton R. N., and Goldsmith J. R. (1996) Oxygen isotope fractionations in muscovite, phlogopite, and rutile. *Geochim. Cosmochim. Acta* **60,** 2595–2608.

Chamberlain C. P. and Conrad M. E. (1991) The relative permeabilities of quartzites and schists during active metamorphism at mid-crustal levels. *Geophys. Res. Lett.* **18,** 959–962.

Chiba C., Chacko T., Clayton R. N., and Goldsmith J. R. (1989) Oxygen isotope fractionations involving diopside, forsterite, magnetite, and calcite: Application to geothermometry. *Geochim. Cosmochim. Acta* **53,** 2985–2995.

Clayton R. N. and Epstein S. (1961) The use of oxygen isotopes in high-temperature geological thermometry. *J. Geol.* **69,** 447–452.

Clayton R. N. and Mayeda T. K. (1963) The use of bromine pentafluoride in the extraction of oxygen from oxides and silicates for isotopic analysis. *Geochim. Cosmochim. Acta* **27,** 43–52.

Clayton R. N., Goldsmith J. R., and Mayeda T. K. (1989) Oxygen isotope fractionation in quartz, albite, anorthite, and calcite. *Geochim. Cosmochim. Acta* **53,** 725–733.

Clayton R. N. and Kieffer S. W. (1991) Oxygen isotope thermometer calibrations. In *Stable Isotope Geochemistry; A Tribute to Samuel Epstein* (ed. H. P. Taylor, Jr. et al.), pp. 3–10.

Clayton R. N. (1993) Oxygen isotopes in meteorites. *Annu. Rev. Earth Planet. Sci.* **21,** 115–149.

Coleman R. G. and Wang X. (1995) Overview of the geology and tectonics of UHPM. In *Ultrahigh Pressure Metamorphism* (ed. R. G. Coleman and X. Wang), pp. 1–32. Cambridge Univ. Press.

Compagnoni R., Hirajima T., and Chopin C. (1995) Ultra-high-pressure metamorphic rocks in the Western Alps. *Ultrahigh Pressure Metamorphism* (ed. R. G. Coleman and X. Wang), pp. 206–243. Cambridge Univ. Press.

Cong B. et al. (1995) Petrogenesis of UHP rocks and their country rocks at Shuanghe in Dabie Shan, central China. *Eur. J. Mineral.* **7,** 119–138.

Cong B. and Wang Q. (1996) A review on researches of UHPM rocks in the Dabieshan-Sulu region. In *Ultrahigh-Pressure Metamorphic Rocks in the Dabieshan-Sulu Region of China* (ed. B. Cong), pp. 1–7. Kluwer Academic Publ.

Coplen T. B. (1995) Reporting of stable carbon, hydrogen, and oxygen isotopic abundances. In *Reference and Intercomparison Materials for Stable Isotopes of Light Elements* (ed. Anonymous), pp. 31–34. IAEA.

Craig H. (1961) Isotopic variations in meteoric waters. *Science* **133,** 1702–1703.

Criss R. E. and Taylor H. P. (1986) Meteoric-hydrothermal systems. In *Stable Isotopes in High Temperature Geological Processes* (ed. J. W. Valley et al.), pp. 373–424. MSA.

Deines P. (1977) On the oxygen isotope distribution among mineral triplets in igneous and metamorphic rocks. *Geochim. Cosmochim. Acta* **41,** 1709–1730.

Desmons J. and O'Neil J. R. (1978) Oxygen and hydrogen isotope compositions of eclogites and associated rocks from the Eastern Sesia Zone (Western Alps, Italy). *Contrib. Mineral. Petrol.* **67,** 79–85.

Eiler J. M., Baumgartner L. P., and Valley J. W. (1992) Intercrystalline stable isotope diffusion: A fast grain boundary model. *Contrib. Mineral. Petrol.* **112,** 543–557.

Eiler J. M., Baumgartner L. P., and Valley J. W. (1994) Fast grain boundary: A Fortran-77 program for calculating the effects of retrograde interdiffusion of stable isotopes. *Comput. Geosci.* **20,** 1415–1434.

Eiler J. M., Valley J. W., Graham C. M., and Baumgartner L. P. (1995) Ion microprobe evidence for the mechanisms of stable isotope retrogression in high-grade metamorphic rocks. *Contrib. Mineral. Petrol.* **118,** 365–378.

Ellis D. J. and Green D. H. (1979) An experimental study of the effect of Ca upon garnet-clinopyroxene Fe-Mg exchange equilibria. *Contrib. Mineral. Petrol.* **71,** 13–22.

Elphick S. C., Graham C. M., and Dennis P. F. (1988) An ion microprobe study of anhydrous oxygen diffusion in anorthite: A comparison with hydrothermal data and some geological implications. *Contrib. Mineral. Petrol.* **100,** 490–495.

Enami M. and Zang Q. (1988) Magnesian staurolite in garnet corundum rocks and eclogite from the Donghai district, Jiangsu province, E China. *Amer. Mineral.* **73,** 48–56.

Enami M. and Zang Q. (1990) Quartz pseudomorph after coesite in eclogites from Shandong province, E. China. *Amer. Mineral.* **75,** 381–386.

Enami M., Zang Q., and Yin Y. (1993) High-pressure eclogites in N Jiangsu – S Shandong province, E China. *J. Metam. Geol.* **11,** 589–603.

Farquhar J., Chacko T., and Ellis D. J. (1996) Preservation of oxygen isotope compositions in granulites from Northwestern Canada and Enderby Land, Antarctica: Implications for high-temperature isotopic thermometry. *Contrib. Mineral. Petrol.* **125,** 213–224.

Farver J. R. and Giletti B. J. (1985) Oxygen diffusion in amphiboles. *Geochim. Cosmochim. Acta* **49,** 1403–1411.

Farver J. R. (1989) Oxygen self-diffusion in diopside with applications to cooling rate determinations. *Earth Planet. Sci. Lett.* **92,** 386–396.

Fortier S. M. and Giletti B. J. (1989) An empirical model for predicting diffusion coefficients in silicate minerals. *Science* **245,** 1481–1484.

Fortier S. M. and Giletti B. J. (1991) Volume self-diffusion of oxygen in biotite, muscovite, and phlogopite micas. *Geochim. Cosmochim. Acta* **55,** 1319–1330.

Ganor J., Matthews A., and Paldor N. (1989) Constraints on effective diffusivity during oxygen isotope exchange at a marble-schist contact, Sifnos (Cyclades), Greece. *Earth Planet. Sci. Lett.* **94,** 208–216.

Ganor J., Matthews A., Schliestedt M., and Garfunkel Z. (1996) Oxygen isotope heterogeneities of metamorphic rocks: An original tectonostratigraphic signature, or an imprint of exotic fluids? A case study of Sifnos and Tinos islands (Greece). *Eur. J. Mineral.* **8,** 719–732.

Gebauer D., Schertl H. P., Brix M., and Schreyer W. (1997) 35 Ma old ultrahigh-pressure metamorphism and evidence for very rapid exhumation in the Dora Maira Massif, western Alps. *Lithos* **41,** 5–24.

Gerdes M. L., Baumgartner L. P., Person M., and Rumble D. (1995) One- and two-dimensional models of fluid flow and stable isotope exchange at an outcrop in the Adamello contact aureole, Southern Alps, Italy. *Amer. Mineral.* **80,** 1004–1019.

Getty S. R. and Selverstone J. (1994) Stable isotope and trace element evidence for restricted fluid migration in 2 GPa eclogites. *J. Metam. Geol.* **12,** 747–760.

Ghent E. D. and Valley J. W. (1998) Oxygen isotope study of quartz-Al_2SiO_5 pairs from the Mica Creek area, British Columbia: Implications for the recovery of peak metamorphic temperatures. *J. Metam. Geol.* **16,** 223–230.

Giletti B. J. (1986) Diffusion effects on oxygen isotope temperatures of slowly cooled igneous and metamorphic rocks. *Earth Planet. Sci. Lett.* **77,** 218–228.

Giletti B. J. and Yund R. A. (1984) Oxygen diffusion in quartz. *J. Geophys. Res.* **89,** 4039–4046.

Godfrey J. D. (1962) The deuterium content of hydrous minerals from the East-Central Sierra Nevada and Yosemite National Park. *Geochim. Cosmochim. Acta* **26,** 1215–1245.

Harley S. L. and Carswell D. A. (1995) Ultradeep crustal metamorphism: A prospective view. *J. Geophys. Res.* **100,** 8367–8380.

Hattori K. and Muehlenbachs K. (1982) Oxygen isotope ratios in the Icelandic crust. *J. Geophys. Res.* **87,** 6559–6565.

Hirajima T., Ishiwatari A., Cong B., Zhang R., Banno S., and Nozaka T. (1990) Coesite from Mengzhong eclogite at Donghai county, NE Jiangsu province China. *Mineral. Mag.* **54,** 579–583.

Hirajima T., Zhang R., Li J., and Cong B. (1992) Petrology of the nyboite bearing eclogite in the Donghai area, Jiangsu province, E. China. *Mineral. Mag.* **56,** 37–46.

Hirajima T., Wallis S. R., Zhai M., and Ye K. (1993) Eclogitized metagranitoid from the Su–Lu ultra-high pressure (UHP) province, Eastern China. *Proc. Japan. Acad.* **69,** Series B, 249–254.

Jamtveit B., Bucher-Nurminen K., and Stijfhoom D. E. (1992) Contact metamorphism of layered shale-carbonate sequences in the Oslo Rift; I, Buffering, infiltration, and the mechanisms of mass transport. *J. Petrol.* **33,** 377–422.

Javoy M. (1977) Stable isotopes and geothermometry. *J. Geol. Soc. London* **133,** 609–636.

Jenkin G. R. T., Farrow C. M., Fallick A. E., and Higgins D. (1994) Oxygen isotope exchange and closure temperatures in cooling rocks. *J. Metam. Geol.* **12,** 221–235.

Kieffer S. W. (1982) Thermodynamics and lattice vibrations of minerals: 5. Applications tp phase equilibria, isotopic fractionation, and high-pressure thermodynamic properties. Rev. Geophys. Space Phys. **20,** 827–849.

Krogh E. J. (1988) The garnet-clinopyroxene Fe-Mg geothermometer: A reinterpretation of existing experimental data. *Contrib. Mineral. Petrol.* **99,** 44–48.

Krogh E. J. and Carswell D. A. (1995) HP and UHP eclogites and garnet peridotites in the Scandinavian Caledonides. In *Ultrahigh Pressure Metamorphism* (ed. R. G. Coleman and X. Wang), pp. 244–298. Cambridge Univ. Press.

Lassey K. R. and Blattner P. (1988) Kinetically controlled oxygen isotope exchange between fluid and rock in one-dimensional advective flow. *Geochim. Cosmochim. Acta* **52,** 2169–2175.

Li S. et al. (1994) Excess Ar in phengite from eclogite: Evidence from dating of eclogite minerals by Sm-Nd, Rb-Sr, and $^{40}Ar/^{39}Ar$ methods. *Chem. Geol.* **112,** 343–350.

Li S. (1996) Isotopic geochronology. In *Ultrahigh-Pressure Metamorphic Rocks in the Dabieshan-Sulu Region of China* (ed. B. Cong), pp. 90–105. Kluwer Academic Publ.

Liou J. G., Zhang R. Y., and Ernst W. G. (1995) Occurrences of hydrous and carbonate phases in ultrahigh-pressure rocks from east-central China: Implications for the role of volatiles deep in cold subduction zones. *Island Arc* **4,** 362–375.

Liou J. G. and Zhang R. Y. (1996) Occurrences of intergranular coesite in ultrahigh-P rocks from the Sulu region, eastern China: Implications for lack of fluid during exhumation. *Amer. Mineral.* **81,** 1217–1221.

Magaritz M. and Taylor H. P. Jr. (1976) Isotopic evidence for meteoric-hydrothermal alteration of plutonic igneous rocks in the Yakutat Bay and Skagway areas, Alaska. *Earth Planet. Sci. Lett.* **30,** 179–190.

Massey J. A., Harmon R. S., and Harris N. B. W. (1994) Contrasting retrograde oxygen isotope exchange behaviour and implications: Examples from the Langtang Valley, Nepal. *J. Metam. Geol.* **12,** 261–272.

Matthews A., Beckinsale R. D., and Durham J. J. (1979) Oxygen isotope fractionation between rutile and water and geothermometry of metamorphic eclogites. *Mineral. Mag.* **43,** 405–413.

Matthews A. (1994) Oxygen isotope geothermometers for metamorphic rocks. *J. Metam. Geol.* **12,** 211–219.

Matthews A., Liata A., Mposkos E., and Skarpelis N. (1996) Oxygen isotope geochemistry of the Rhodope polymetamorphic terrain in northern Greece: Evidence for preservation of pre-metamorphic isotopic compositions. *Eur. J. Mineral.* **8,** 1139–1152.

Michard A., Henry C., and Chopin C. (1995) Structures in UHPM rocks: A case study from the Alps. In *Ultrahigh Pressure Metamorphism* (ed. R. G. Coleman and X. Wang), pp. 132–158. Cambridge Univ. Press.

Moore D. K., Cherniak D. J., and Watson E. B. (1998) Oxygen diffusion in rutile from 750° to 1000°C and 0.1 to 1000 MPa. *Amer. Mineral.* **83,** 700–711.

Nevle R. J., Brandriss M. E., Bird D. K., McWilliams M. O., and O'Neil J. R. (1994) Tertiary plutons monitor climate change in East Greenland. *Geology* **22,** 775–778.

Nickel K. G. and Green D. H. (1985) Empirical geothermobarometry for garnet peridotites and implications for the nature of the lithosphere, kimberlites, and diamonds. *Earth Planet. Sci. Lett.* **73,** 158–170.

O'Neill H. S. and Wood B. J. (1980) An experimental study of Fe-Mg partitioning between garnet and olivine and its calibration as a geothermometer: Corrections. *Contrib. Mineral. Petrol.* **72,** 337

Powell R. (1985) Regression diagnostic and robust regression in geothermometer / geobarometer calibration: The garnet-clinopyroxene geothermometer revisited. *J. Metam. Geol.* **3,** 231–243.

Rosenbaum J. M. and Mattey D. (1995) Equilibrium garnet-calcite oxygen isotope fractionation. *Geochim. Cosmochim. Acta* **59,** 2839–2842.

Rowley D. B., Xue F., Tucker R. D., Peng Z. X., Baker J., and Davis A. (1997) Ages of ultrahigh pressure metamorphism and protolith orthogneisses from the eastern Dabie Shan: U/Pb zircon geochronology. *Earth Planet. Sci. Lett.* **151,** 191–203.

Rumble D. (1973) Fe-Ti oxide minerals from regionally metamorphosed quartzites of Western New Hampshire. *Contrib. Mineral. Petrol.* **42,** 181–195.

Rumble D. (1978) Mineralogy, petrology, and oxygen isotopic geochemistry of the Clough Formation, Black Mountain, Western New Hampshire, USA. *J. Petrol.* **19,** 317–340.

Rumble D. and Spear F. S. (1983) Oxygen-isotope equilibration and permeability enhancement during regional metamorphism. *J. Geol. Soc. London* **140,** 619–628.

Rumble D. and Hoering T. C. (1994) Analysis of oxygen and sulfur isotopes ratios in oxide and sulfide minerals by spot heating with a carbon dioxide laser in a fluorine atmosphere. *Acc. Chem. Res.* **27,** 237–241.

Rumble D. (1994) Water circulation in metamorphism. *J. Geophys. Res.* **99,** 15499–15502.

Rumble D., Farquhar J., Young E. D., and Christensen C. P. (1997) In situ oxygen isotope analysis with an excimer laser using F_2 and BrF_5 reagents and O_2 gas as analyte. *Geochim. Cosmochim. Acta* **61,** 4229–4234.

Schreyer W. (1995) Ultradeep metamorphic rocks: The retrospective viewpoint. *J. Geophys. Res.* **100,** 8353–8366.

Sharp Z. D. (1990) A laser-based microanalytical method for the in situ determination of oxygen isotope ratios of silicates and oxides. *Geochim. Cosmochim. Acta* **54,** 1353–1357.

Sharp Z. D., Giletti B. J., and Yoder H. S., Jr. (1991) Oxygen diffusion rates in quartz exchanged with CO_2. *Earth Planet. Sci. Lett.* **107,** 339–348.

Sharp Z. D., Essene E. J., and Hunziger J. C. (1993) Stable isotope geochemistry and phase equilibria of coesite-bearing whiteschists, Dora Maira massif, western Alps. *Contrib. Mineral. Petrol.* **114,** 1–12.

Sharp Z. D. and Kirschner D. L. (1994) Quartz-calcite oxygen isotope geothermometry: A calibration based on natural isotopic variations. *Geochim. Cosmochim. Acta* **58,** 4491–4501.

Sharp Z. D. and Moecher D. P. (1994) Oxygen isotope variations in a porphyroclastic meta–anorthosite: Diffusion effects and false isotherms. *Amer. Mineral.* **79,** 951–959.

Sharp Z. D. (1995) Oxygen isotope geochemistry of the Al_2SiO_5 polymorphs. *Amer. J. Sci.* **295,** 1058–1076.

Sheppard S. M. F. and Schwarcz H. P. (1970) Fractionation of carbon and oxygen isotopes and magnesium between coexisting metamorphic calcite and dolomite. *Contrib. Mineral. Petrol.* **26,** 161–198.

Sheppard S. M. F. and Taylor H. P., Jr. (1974) Hydrogen and oxygen isotope evidence for the origin of water in the Boulder batholith and the Butte ore deposits. *Econ. Geol.* **69,** 926–946.

Smith D.C. (1995) Microcoesites and microdiamonds in Norway. In *Ultrahigh Pressure Metamorphism* (ed. R. G. Coleman and X. Wang), pp. 299–355. Cambridge Univ. Press.

Taylor H. P., Jr. and Coleman R. G. (1968) $^{18}O/^{16}$ ratios of coexisting minerals in glaucophane-bearing metamorphic rocks. *Geol. Soc. Amer. Bull.* **79,** 1727–1755.

Taylor H. P., Jr. (1974) The application of oxygen and hydrogen isotope studies to problems of hydrothermal alteration and ore deposition. *Econ. Geol.* **69,** 843–883.

Tilton G. R., Ames L., Schertl H. P., and Schreyer W. (1997) Reconnaissance isotopic investigations on rocks of an undeformed granite contact within the coesite-bearing unit of the Dora Maira Massif. *Lithos* **41,** 25–36.

Todd C. S. and Evans B. W. (1993) Limited fluid–rock interaction at marble-gneiss contacts during Cretaceous granulite-facies metamorphism, Seward Peninsula, Alaska. *Contrib. Mineral. Petrol.* **114,** 27–41.

Vogel D. E. and Garlick G. D. (1970) Oxygen-isotope ratios in metamorphic eclogites. *Contrib. Mineral. Petrol.* **28,** 183–191.

Wang Q. et al. (1993) Coesite-bearing granulite retrograded from eclogite in Weihai, eastern China. *Eur. J. Mineral.* **5,** 141–152.

Wang Q. Liu X., Zhao Z., and Chen J. (1996) Structural Geology. In *Ultrahigh-Pressure Metamorphic Rocks in the Dabieshan-Sulu Region of China* (ed. B. Cong), pp. 27–48. Kluwer Academic Publ.

Wang X., Zhang R., and Liou J. G. (1995) UHPM terrane in E central China. In *Ultrahigh Pressure Metamorphism* (ed. R. G. Coleman and X. Wang), pp. 356–390. Cambridge Univ. Press.

Watson E. B. and Cherniak D. J. (1997) Oxygen diffusion in zircon. *Earth Planet. Sci. Lett.* **148,** 527–544.

Wickham S. M. and Peters M. T. (1992) Oxygen and carbon isotope profiles in metasediments from Lizzies Basin, East Humboldt Range, Nevada; constraints on mid-crustal metamorphic and magmatic volatile fluxes. *Contrib. Mineral. Petrol.* **112,** 46–65.

Wiechert U. and Hoefs J. (1995) An excimer laser-based micro analytical preparation technique for in situ oxygen isotope analysis of silicate and oxide minerals. *Geochim. Cosmochim. Acta* **59,** 4093–4101.

Xu J. (1993) Basic characteristics and tectonic evolution of the Tanchung-Lujiang fault zone. In *The Tancheng-Lujiang Wrench Fault System* (ed. J. Xu), pp. 17–50. Wiley.

Xu Y. G., Menzies M. A., Mattey D., Lowry D., Harte B., and Hinton R. W. (1996) The nature of the lithospheric mantle near the Tancheng-Lujiang fault, China: An integration of texture, chemistry, and oxygen isotopes. *Chem. Geol.* **134,** 67–82.

Xue F., Rowley D. B., and Baker J. (1996) Refolded syn-ultrahigh-pressure thrust sheets in the south Dabie complex, China: Field evidence and tectonic implications. *Geology* **24,** 455–458.

Yang J. and Smith D. C. (1989) Evidence for a former sanidine-coesite-eclogite at Lanshantou, east China, and the recognition of a Chinese ‘Su-Lu coesite-eclogite province’. In *Third International Eclogite Conference* (ed. Anonymous), pp. 26. Blackwell Sci. Publ.

Yang J., Godard G., Kienast J. R., Lu Y., and Sun J. (1993) Ultrahigh-Pressure (60 Kbar) magnesite-bearing garnet peridotite from Northeastern Jiangsu, China. *J. Geol.* **101,** 541–554.

Ye K., Hirajima T., Ishiwatari A., Gou J., and Zhai M. (1996) The discovery of intergranular coesite in eclogite from Yangkou, Qingdao. *Chinese Sci. Bull.* **41,** 1407–1408.

Yui T. Z., Rumble D., and Lo C. H. (1994) Stable-isotope characteristics of the ultra-high pressure (UHP) metamorphic rocks of China. In *First Workshop on UHP Metamorphism* (ed. J. G. Liou et al.), pp. A-76–A-77 Stanford Univ Press.

Yui T. Z., Rumble D., and Lo C. H. (1995) Unusually low $\delta^{18}O$ ultrahigh-pressure metamorphic rocks from the Sulu terrain, eastern China. *Geochim. Cosmochim. Acta* **59,** 2859–2864.

Yui T. Z., Rumble D., Chen C. H., and Lo C. H. (1997) Stable isotope characteristics of eclogites from the ultra-high-pressure metamorphic terrain, east-central China. *Chem. Geol.* **137,** 135–147.

Zhang R. Y., Liou J. G., and Cong B. (1994) Petrogenesis of garnet - bearing ultramafic rocks and associated eclogites in the Su Lu UHP metamorphic terrane, E China. *J. Metam. Geol.* **12,** 169–186.

Zhang R. Y., Liou J. G., and Ernst W. G. (1995) Ultrahigh-pressure metamorphism and decompression P-T paths of eclogites and country rocks from Weihai, eastern China. *Island Arc* **4,** 293–309.

Zhang R. Y., Hirajima T., Banno S., Cong B., and Liou J. G. (1995) Petrology of ultrahigh-pressure rocks from the southern Su-Lu region, eastern China. *J. Metam. Geol.* **13,** 659–675.

Zhang R. Y. and Liou J. G. (1997) Partial transformation of gabbro to coesite-bearing eclogite from Yangkou, the Sulu terrane, eastern China. *J. Metam. Geol.* **15,** 183–202.

Zheng Y. F. (1991) Calculation of oxygen isotope fractionation in metal oxides. *Geochim. Cosmochim. Acta* **55,** 2299–2307.

Zheng Y. F. (1993) Calculation of oxygen isotope fractionation in hydroxyl-bearing silicates. *Earth Planet. Sci. Lett.* **120,** 247–263.

Zheng Y. F. (1993) Calculation of oxygen isotope fractionation in anhydrous silicate minerals. *Geochim. Cosmochim. Acta* **57,** 1079–1091.

Zheng Y. F., Metz P., Satir M., and Sharp Z. D. (1994) An experimental calibration of oxygen isotope fractionation between calcite and forsterite in the presence of a CO_2–H_2O fluid. *Chem. Geol.* **116,** 17–27.

Zheng Y. F., Fu B., Gong B., and Li S. (1996) Extreme ^{18}O depletion in eclogite from the Su-Lu terrane in east China. *Eur. J. Mineral.* **8,** 317–323.

Zheng Y. F., Fu B., Li Y., Xiao Y., and Li S. (1998) Oxygen and hydrogen isotope geochemistry of ultrahigh-pressure eclogites from the Dabie Mountains and the Sulu terrane. *Earth Planet. Sci. Lett.* **155,** 113–129.